Supporting Information

Molecular conformation: A key factor underlying the performances of heterojunction photocatalysts

Wanyu Liang,[a] Ruyue Jiang,[a] Xiao Tian,[a] Hantang Zhang,*[a] Bowen Zhang,*[ab] Xiuqiang Lu,*[c] Jie Liu,[d] Lang Jiang,[d] Shifeng Hou,[a] Shiyun Ai [a]

[a]College of Chemistry and Material Science, Key Laboratory of Agricultural Film Application of Ministry of Agriculture and Rural Affairs, Shandong Agriculture University; TaiAn 271018, P. R. China.

[b]Department of Chemistry, Texas A&M University, College Station, Texas 77843, United States.

[c]School of Materials and Packaging Engineering, Fujian Polytechnic Normal University, Fuqing, Fujian 350300, P. R. China.

[d]Beijing National Laboratory for Molecular Sciences, Key Laboratory of Organic Solids, Institute of Chemistry, Chinese Academy of Science, Beijing 100190, P. R. China

*Corresponding author
E-mail: htzhang@sdau.edu.cn (Hantang Zhang); bowenzhang@sdau.edu.cn (Bowen Zhang); luxiuqiang@iccas.ac.cn (Xiuqiang Lu)

Experimental Section

Synthesis of carbon nitride nanosheets

The pristine carbon nitride was synthesized by thermal condensation in air. An appropriate amount of precursor-urea was placed in a sealed crucible and heated to 550 °C at a rate of 3 °/min. Maintain at 550 °C for 4 hours, then cool to room temperature. Bulk CN obtained by this step.

Carbon nitride nanosheets obtained by two-step method. First, the lumpy carbon nitride obtained from the initial calcination is placed in an open crucible and fully exposed to air. Next, heat to 520 °C at 5 °/min and maintain for 2 hours. The carbon nitride obtained by secondary calcination was dispersed into the isopropanol solution and the carbon nitride nanosheets were obtained by high power sonication at 500 W for 10 h.

Synthesis of CuTPP and CuTBPP

Synthesis of CuTPP: Mix benzaldehyde (3.2 g, 0.03 mmol) and pyrrole (2.0 g, 0.03 mmol) evenly, slowly add to slightly boiling propionic acid (100 mL), reflux and stir for 30 minutes, and stop the reaction. Allow the reaction solution to cool to room temperature, add ethanol (20 mL), and freeze in the refrigerator. Filter with a Buchner funnel, wash the filter cake with hot water and methanol in sequence until the filtrate is clear. The obtained free alkali porphyrin compound (H_2TPP) was dried to obtain a purple solid product (0.92 g, 20%).

H_2TPP (500 mg, 0.814 mmol, 1.0 equiv) and $Cu(OAc)_2 \cdot H_2O$ (5.0 equiv) were heated and refluxed in DMF (50 mL) for about 1 hour. The reaction was stopped, cooled to room temperature, and water (50 mL) was added. At this point, a large amount of product precipitated. The product CuTPP (551 mg, 100%) was obtained by suction filtration with a Buchner funnel, washing the filter cake with water, and drying.

Synthesis of CuTBPP: Dissolve dipyrrolemethane (2.19 g, 15 mmol, 1.0 equiv) and aryl formaldehyde (3.27 g, 15 mmol, 1.0 equiv) in dichloromethane (1500 mL, analytically pure), add trifluoroacetic acid (2.06 mL, 26.7 mmol, 1.78 equiv) under dark conditions, stir at room temperature for 3 hours, then add DDQ (3.41 g, 15 mmol, 1.0 equiv) for oxidation, continue stirring for 1 hour, and add triethylamine (15 mL) to the system for neutralization. After the reaction solution is concentrated to about 1/3 volume, a dry silica gel column is used to collect the purple red band containing the product, and the product free base porphyrin (2.06 g, 40%, denoted as H_2TBPP) is recrystallized (dichloromethane/methanol,V/V = 1:1).

H_2TBPP (560 mg, 0.814 mmol, 1.0 equiv) and $Cu(OAc)_2 \cdot H_2O$ (5.0 equiv) were heated and refluxed in DMF (50 mL) for about 1 hour. The reaction was stopped, cooled to room temperature, and water (50 mL) was added. At this point, a large amount of product precipitated.

The product CuTBPP (609 mg, 100%) was obtained by suction filtration with a Buchner funnel, washing the filter cake with water, and drying.

Preparation of CuPy/CN heterojunction photocatalysts

An amount of CuPy (7 wt.%) was added to the isopropanol suspension of CN. The mixed suspensions were sonicated at low power for 2 hours. The mixed suspensions were centrifuged at 3500 r/min for 5 min. The CuPy/CN heterojunction photocatalysts were obtained by decanting the upper clear layer.

Photocatalytic hydrogen evolution experiments

20 mg of photocatalyst and 50 mL of ultrapure water were added to the reactor. 5 wt.% Pt was loaded onto the catalyst surface as a co-catalyst by photodeposition of $H_2PtCl_6 \cdot 6H_2O$. 10 vol.% triethanolamine (TEOA) was used as a cavity sacrificial agent. N_2 was introduced into the mixture for 30 minutes to remove the air before the light. The photocatalytic hydrogen production experiments were performed under 300W as the light source and circulating condensed water (6 °C). The amount of hydrogen was analyzed by gas chromatograph. The instrument is equipped with a thermal conductivity detector (TCD).

Computational methods

Density functional theory calculations were performed with Gaussian 16 C01.[1] The density functional and basis sets were selected to be B3LYP[2-4]-GD3BJ[5,6]/def2-TZVP for Cu and def2SVP for other atoms[7]. Implicit Solvation Model based on Density (SMD) was used,[8] and water was selected as the continuum. The Wavefunction analyses were performed with Multiwfn 3.8 (dev).[9,10] The ESP evaluation code based on LIBRETA library[11] was utilized in producing Fig. 6. A $C_{36}N_{49}H_3$ molecule (Fig. S13) was used to model the CN layer.

Cyclic Voltammetry test of ferrocene/ferrocenium ($Fc^{0/+}$), CuTPP and CuTBPP

A concentration of 10^{-5} M was dissolved in dry CH_2Cl_2 and 0.1 M Bu_4NPF_6 was used as the supporting electrolyte. Ferrocene is used as an external standard. CV was tested using a three-electrode system, with Ag/AgCl as the reference electrode.

The oxidation energy level of ferrocene under vacuum conditions is -4.8 eV. The HOMO and LUMO energy levels of the material are calculated by the following empirical equations : $E_{HOMO} = - (E_{ox} + 4.8)$ eV, $E_{LUMO} = E_{HOMO} + E_g$. E_{ox} is the difference between the starting oxidation potential of the material and ferrocene. E_g is the optical energy level bandwidth of the material, obtained from the UV-visible spectrum.

Mott-Schottky test of CN

0.5 M of Na_2SO_4 solution was used as the electrolyte. 2 mg/mL of CN was dropped onto glassy carbon electrode and baked dry with an infrared lamp. The Mott-Schottky test was performed

using a three-electrode system in which a saturated glycoelectrode was used as the reference electrode.

EIS of CN, CuTPP/CN and CuTBPP/CN heterojunction

The same concentration of $[Fe(CN)_6]^{3-}$ and $[Fe(CN)_6]^{4-}$ (5 mM) containing 0.1 M KCl was used as the electrolyte. A 2 mg/mL suspension of CN (or CuTPP/CN or CuTBPP/CN) isopropanol was dropped onto glassy carbon electrode, respectively, and baked dry with an infrared lamp. The EIS was tested using a three-electrode system with a saturated glycoelectrode as the reference electrode.

Photocurrent response of CN, CuTPP/CN and CuTBPP/CN heterojunction

0.5 M Na_2SO_4 solution was used as the electrolyte. A 2 mg/ml suspension of CN (or CuTPP/CN or CuTBPP/CN) isopropanol was dropped onto the ITO electrode and baked dry with an infrared lamp. An LED white light is used as the light source. Photocurrent response was tested using a three-electrode system in which a Saturated glyco-electrode was used as the reference electrode.
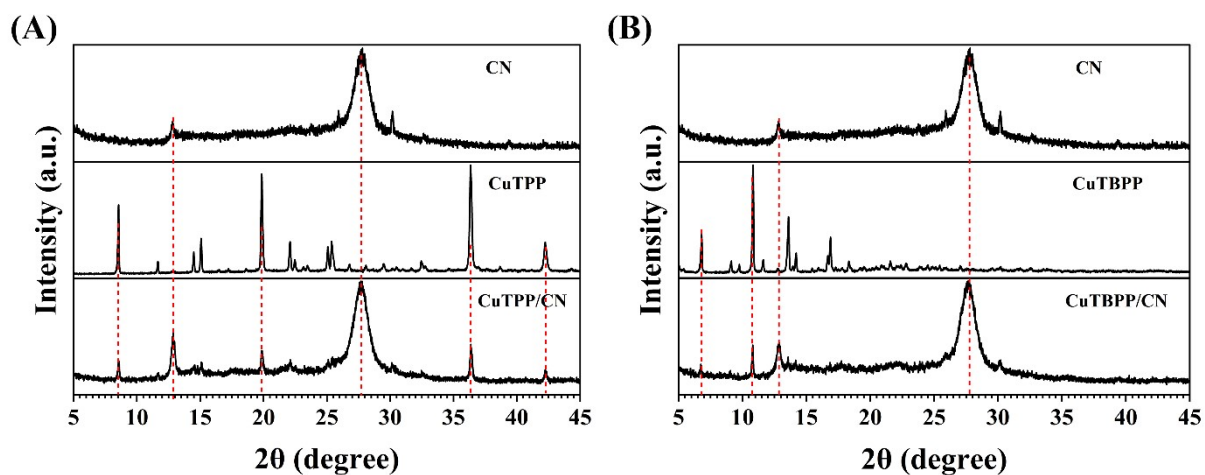
Fig. S1 (A) XRD of CN, CuTPP and CuTPP/CN (7 wt.%) heterojunctions. (B) XRD of CN, CuTBPP and CuTBPP/CN (7 wt.%) heterojunctions.
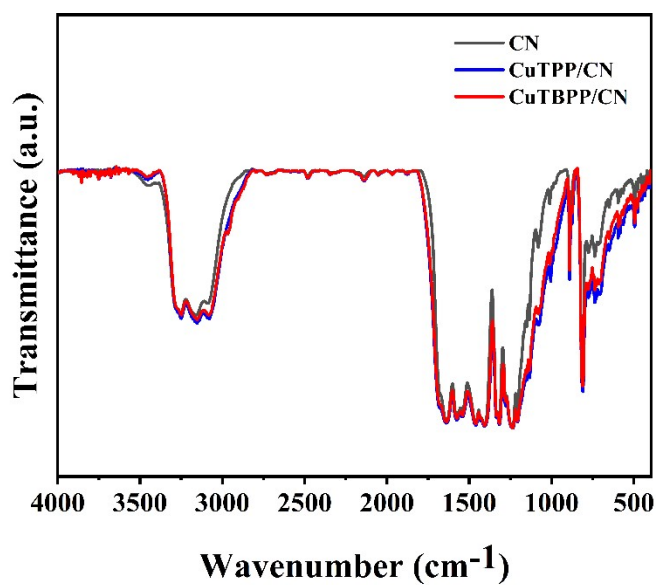
Fig. S2 FTIR of CN, CuTPP/CN (7 wt.%) and CuTBPP/CN (7 wt.%) heterojunctions. The weight of CN is the same in different samples.
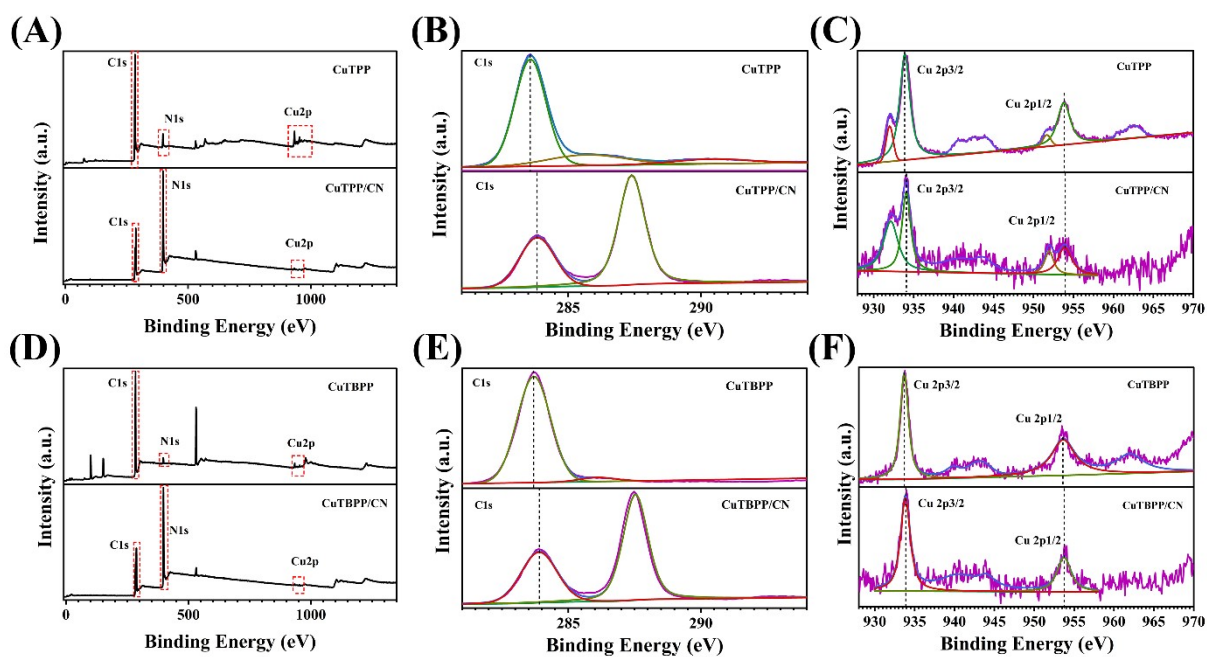
Fig. S3 Broad XPS scan of (A) CuTPP, CuTPP/CN (7 wt.%) heterojunctions and (D) CuTBPP, CuTBPP/CN (7 wt.%) heterojunctions. C 1s XPS of (B) CuTPP, C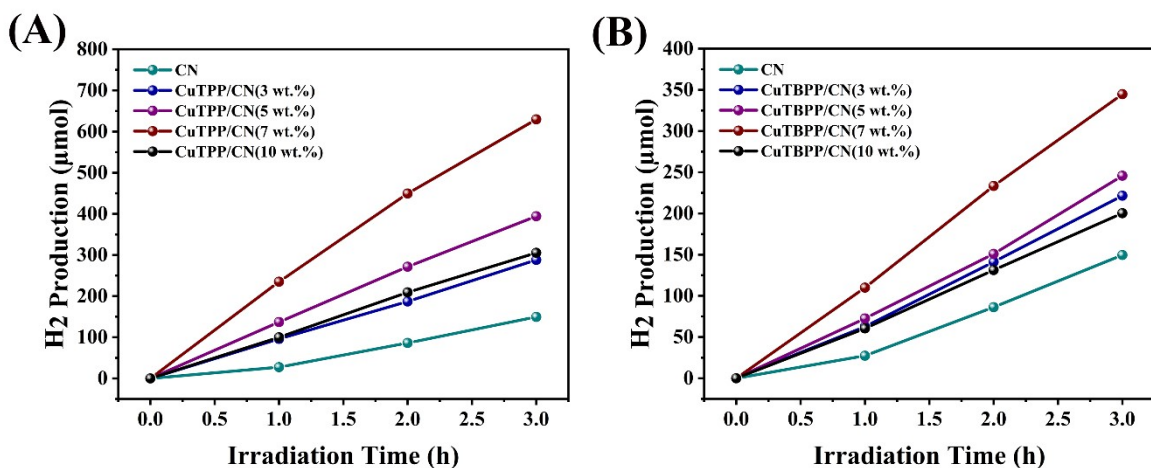uTPP/CN (7 wt.%) heterojunctions and (E) CuTBPP, CuTBPP/CN (7 wt.%) heterojunctions. Cu 2p XPS of (C) CuTPP, CuTPP/CN (7 wt.%) heterojunctions and (F) CuTBPP, CuTBPP/CN (7 wt.%) heterojunctions.

Fig. S4 PHE measurements of CuTPP/CN and CuTBPP/CN heterojunctions measured under the irradiation of a 300 W Xenon lamp. TEOA is used as the hole sacrificial agent. 5 wt.% Pt is used as a cocatalyst.
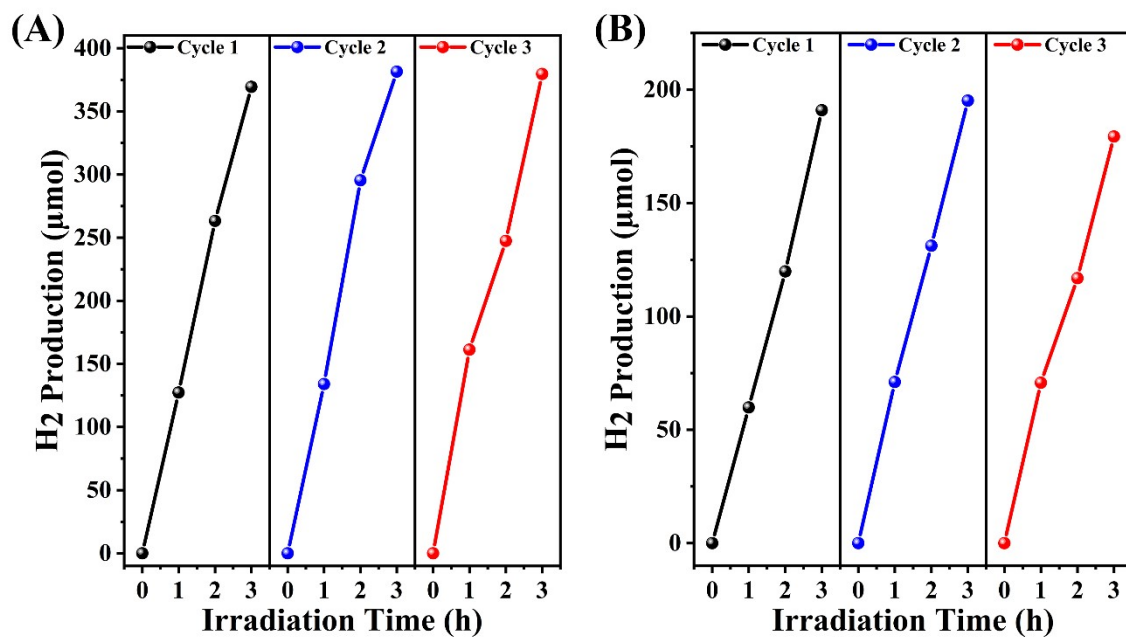
Fig. S5 Cycling test of (A) CuTPP/CN (7 wt.%) and (B) CuTBPP/CN (7 wt.%) heterojunctions.
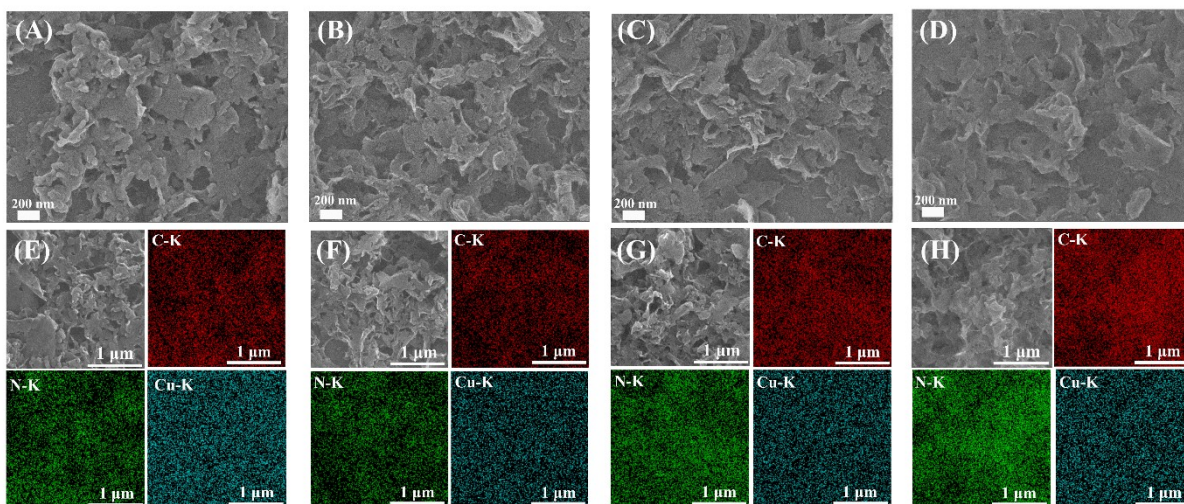
Fig. S6 Scanning electron microscope (SEM) image of (A) CuTPP/CN (7 wt.%) and (C) CuTBPP/CN (7 wt.%) heterojunctions before reaction. Electron image before reaction and the corresponding SEM-assisted elemental mapping of C, N and Cu of (E) CuTPP/CN (7 wt.%) and (G) CuTBPP/CN (7 wt.%) composite. Scanning electron microscope (SEM) image of (B) CuTPP/CN (7 wt.%) and (D) CuTBPP/CN (7 wt.%) heterojunctions after reaction. Electron image after reaction and the corresponding SEM-assisted elemental mapping of C, N and Cu of (f) CuTPP/CN (7 wt.%) and (H) CuTBPP/CN (7 wt.%) composite.
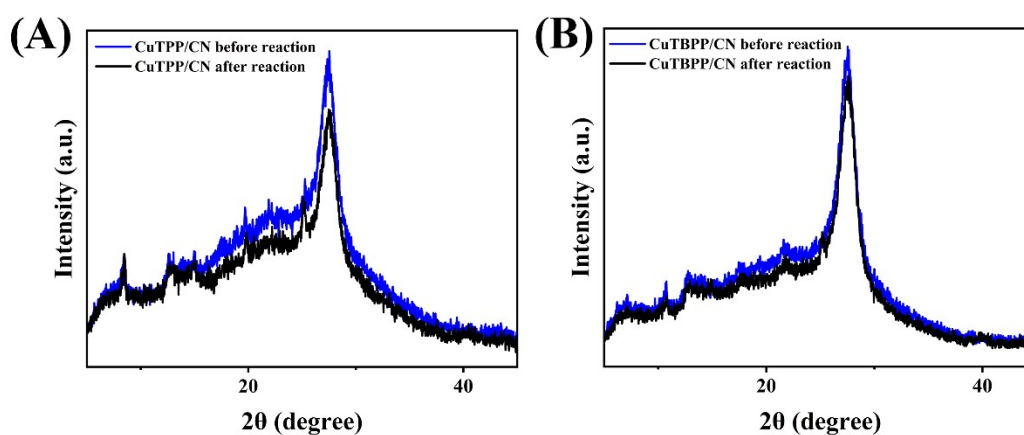
Fig. S7 (A) XRD of CuTPP/CN (7 wt.%) heterojunctions before and after the reaction. (B) XRD of CuTBPP/CN (7 wt.%) heterojunctions before and after the reaction.
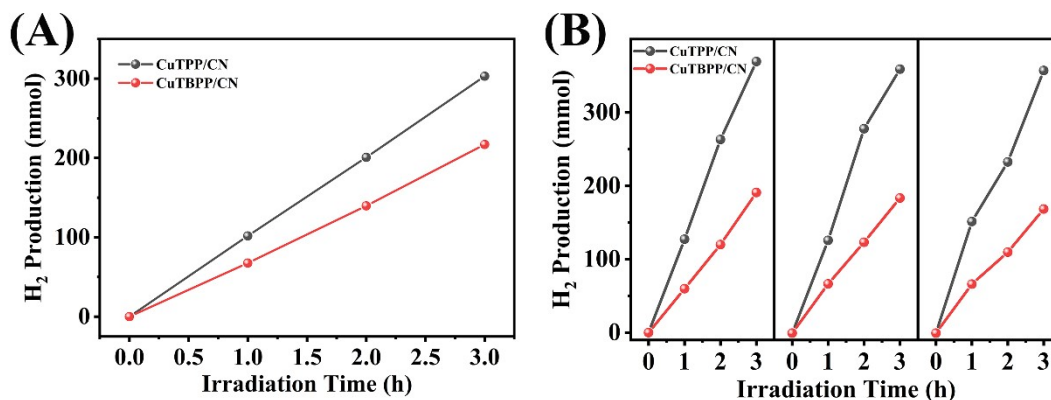
Fig. S8 (A) Repeated PHE test of CuTPP/CN (7 wt.%) and CuTBPP/CN (7 wt.%) heterojunctions. (B) Comparison of PHE performances of CuTPP/CN (7 wt.%) and CuTBPP/CN (7 wt.%) heterojunctions during the cycling test.
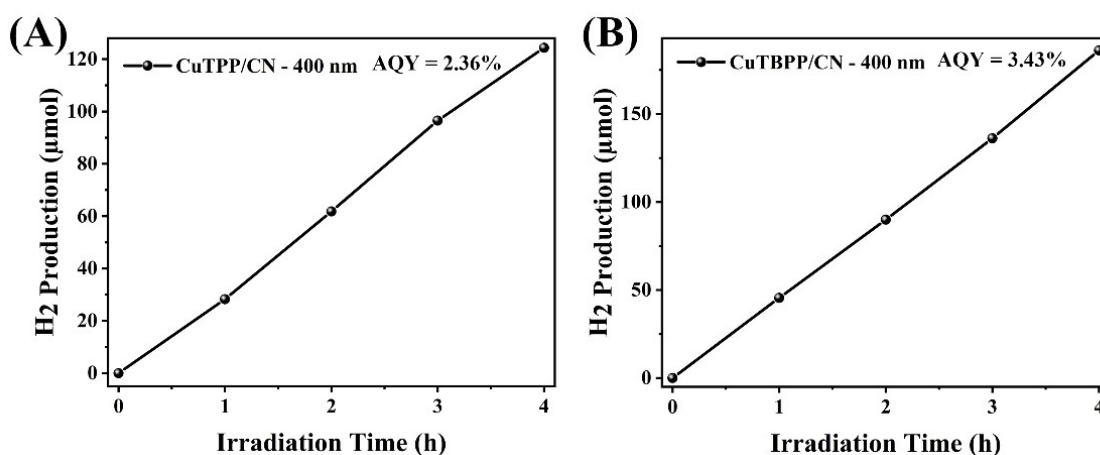

Fig. S9 PHE test of CuTPP/CN (7 wt.%) and CuTBPP/CN (7 wt.%) heterojunctions under 400nm.

The AQY of CuTBPP/CN is higher than that of CuTPP/CN at 400nm, which may result from the different light absorption of the samples at 400nm. As depicted in Fig. S10A and B, CuTBPP has stronger solid-state light absorption at 400 nm than CuTPP, as the case for both heterojunctions. To confirm this result, CuTBPP and CuTPP's single-molecule absorption were also conducted, with extremely dilute solutions of the same concentration (Fig. S10C). It shows that CuTPP has barely absorption at 400nm. Despite the better AQY of CuTBPP/CN at 400nm, the PHE performances of CuTPP/CN does outperform that of CuTBPP/CN in the entire visible spectral range, as demonstrated in Fig. S8.
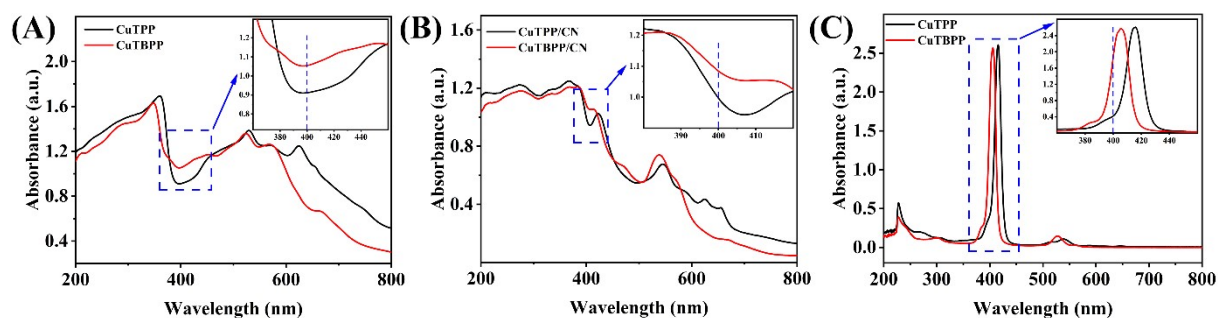
Fig. S10 (A) DRS of CuTPP and CuTBPP. (B) DRS of CuTPP/CN (7 wt.%) and CuTBPP/CN (7 wt.%) heterojunctions. (C) UV−vis absorption spectra of CuTPP and CuTBPP CH$_2$Cl$_2$ solution of the same concentration.
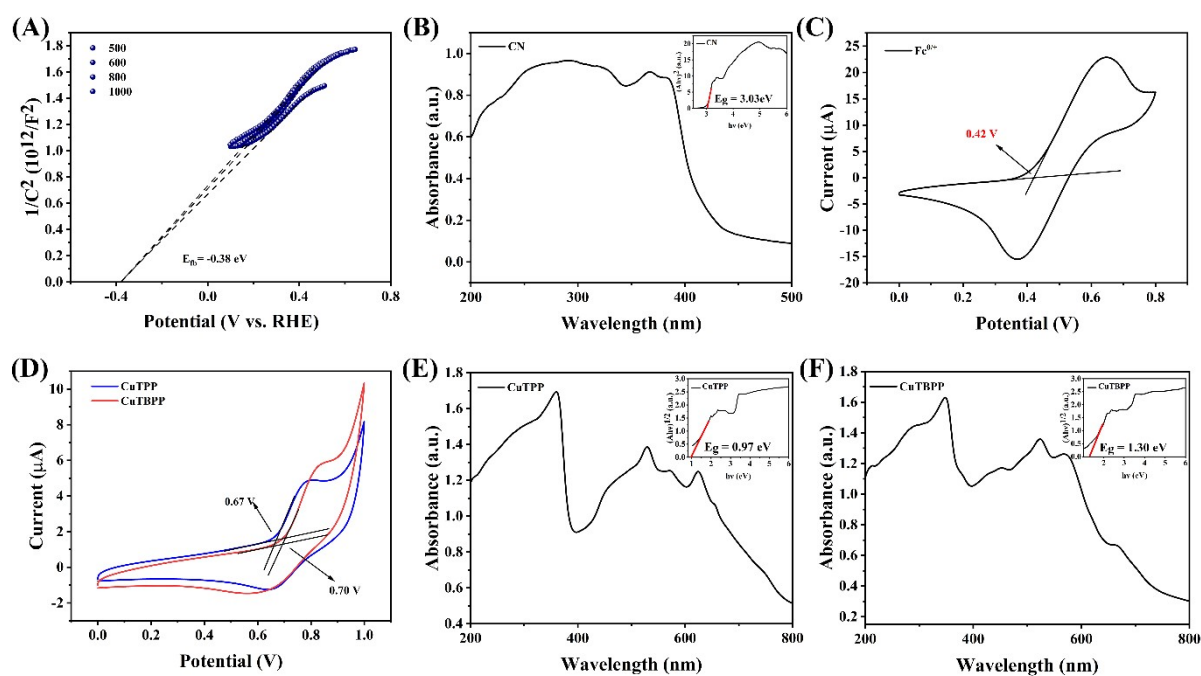

Fig. S11 (A) Mott-Schottky plot of CN. DRS of (B) CN (inset) corresponding Tacu plots. (C) Cyclic voltammograms curves of ferrocene/ferrocenium (Fc$^{0/+}$) redox couple. (D) Oxidative half cyclic voltammograms to determine the HOMO positions of CuTPP and CuTBPP. DRS of (E) CuTPP and (F) CuTBPP, (inset) corresponding Tacu plots.

Table S1 DFT calculated interaction energies ΔE (electronic energy) of CN with CuTPP and CuTBPP at different distances. The optimum interaction is shown in bold

distance (Å) *	CuTPP + CN		CuTBPP + CN	
	ΔE (kcal/mol)	distortion energy (kcal/mol) **	ΔE (kcal/mol)	distortion energy (kcal/mol) **
2.8	-121.03	20.12	-117.42	21.54
2.9	-127.14	18.63	-120.89	19.72
3.0	-130.38	17.09	-123.02	17.45
3.1	-132.32	15.24	-125.55	15.72
3.2	-132.58	13.76	-127.19	15.39
3.3	-133.55	13.08	**-127.24**	**14.74**
3.4	-133.66	12.55	-126.85	15.06
3.5	**-133.92**	**12.00**	-126.62	15.71
3.6	-133.81	11.57	-125.87	16.41
3.7	-132.84	10.37	-123.48	17.22

* "Distance" is defined as the distance between the copper atom and the geometric center of the CN model.

** "Distortion energy" is defined as the electronic energy difference between the frozen CuTPP (CuTBPP) moiety (also called "distorted geometry" in later sections) from the CuTPP (CuTBPP) + CN adduct with the fully relaxed CuTPP (CuTBPP) molecule.

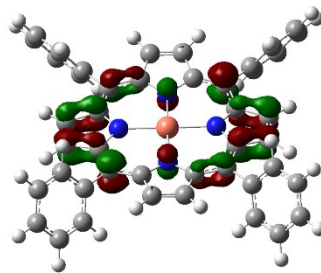**Table S2** Calculated electron affinity of CuTPP and CuTBPP

	Vertical electron affinity (eV)	Vertical electron affinity (Distorted geometry*, eV)	Adiabatic electron affinity (eV)
CuTPP	-2.42	-2.56	-2.59
CuTBPP	-2.36	-2.40	-2.53

* Distorted geometry: see definition in the above section
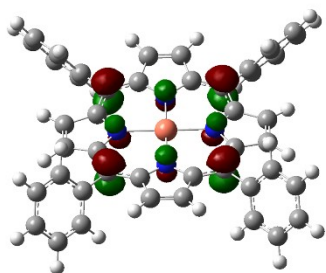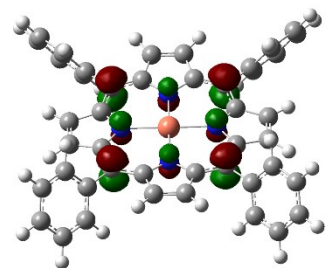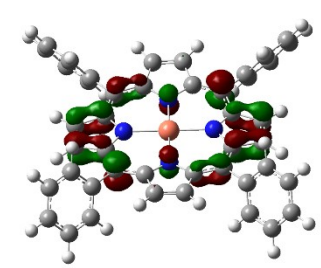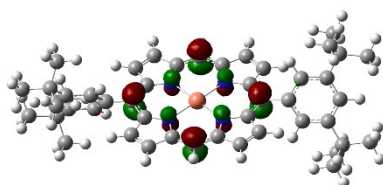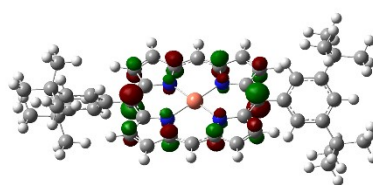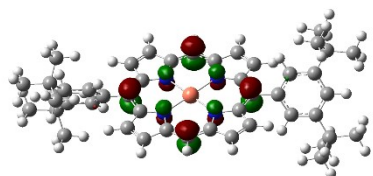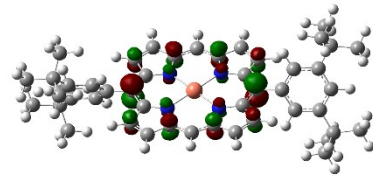
Fig. S12 B3LYPBS (BS = def2-TZVP for Cu and def2-SVP for other atoms) wave functions of the frontier molecular orbital in CuTPP and CuTBPP. The grey ball: carbon atom; blue ball: nitrogen atom; yellow ball: copper atom; white ball: hydrogen atom.
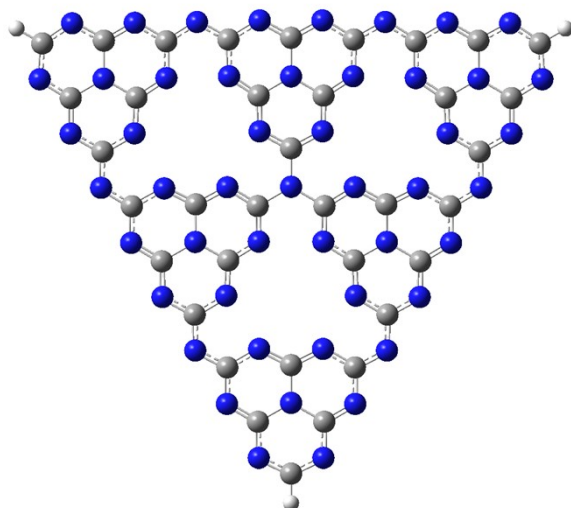
Fig. S13 Structure of the CN molecular model ($C_{36}N_{49}H_3$).

References

1 M. e. Frisch, G. Trucks, H. Schlegel, G. Scuseria, M. Robb, J. Cheeseman, G. Scalmani, V. Barone, G. Petersson and H. Nakatsuji, Gaussian 16, revision C. 01. Gaussian, Inc., Wallingford CT: 2016.

2 A. D. Becke, *J. Chem. Phys.*, 1993, **98**, 5648−5652.

3 S. H. Vosko, L. Wilk and M. Nusair, *Canadian Journal of physics*, 1980, **58**, 1200-1211.

4 P. J. Stephens, F. J. Devlin, C. F. Chabalowski and M. J. Frisch, *The Journal of physical chemistry*, 1994, **98**, 11623-11627.

5 S. Grimme, J. Antony, S. Ehrlich and H. Krieg, *The Journal of chemical physics*, 2010, **132**, DOI: 10.1063/1.3382344.

6 S. Grimme, S. Ehrlich and L. Goerigk, *J. Comput. Chem.*, 2011, **32**, 1456-1465.

7 F. Weigend and R. Ahlrichs, *Phys. Chem. Chem. Phys.*, 2005, **7**, 3297-3305.

8 A. V. Marenich, C. J. Cramer and D. G. Truhlar, *The Journal of Physical Chemistry B*, 2009, **113**, 6378-6396.

9 T. Lu and F. Chen, *J. Comput. Chem.*, 2012, **33**, 580-592.

10 T. Lu and F. Chen, *J. Mol. Graphics Modell.*, 2012, **38**, 314-323.

11 J. Zhang and T. Lu, *Phys. Chem. Chem. Phys.*, 2021, **23**, 20323-20328.